Journal of Physics: Conference Series

PAPER • OPEN ACCESS

Features of formation and evolution of crystal and local structures in nanocrystalline $Ln_2Zr_2O_7$ (Ln = La - Tb)

To cite this article: V V Popov *et al* 2017 *J. Phys.: Conf. Ser.* **941** 012079

View the article online for updates and enhancements.

You may also like

- Preparation of Structural Phase Diagram of $Ln_2Ni_{1-x}Cu_xO_{4+\delta}$ (Ln=La, Pr, Nd, Sm, Eu) as New Cathode Materials: Variation of Structural Phase Diagram on Kinds of Ln
Haruki Soga, Chengkun Wang, Tomoki Hayashi et al.
- Structures, magnetic and dielectric properties of the ordered double perovskites $LnPbNiSbO_6$ (Ln = La, Pr)
Lin Han, Yijia Bai, Xiaojuan Liu et al.
- Electrochemical Properties of $Ln(Sr,Ca)_3(Fe,Co)_3O_{10} + Gd_{0.2}Ce_{0.8}O_{1.9}$ Composite Cathodes for Solid Oxide Fuel Cells
Y. N. Kim and A. Manthiram

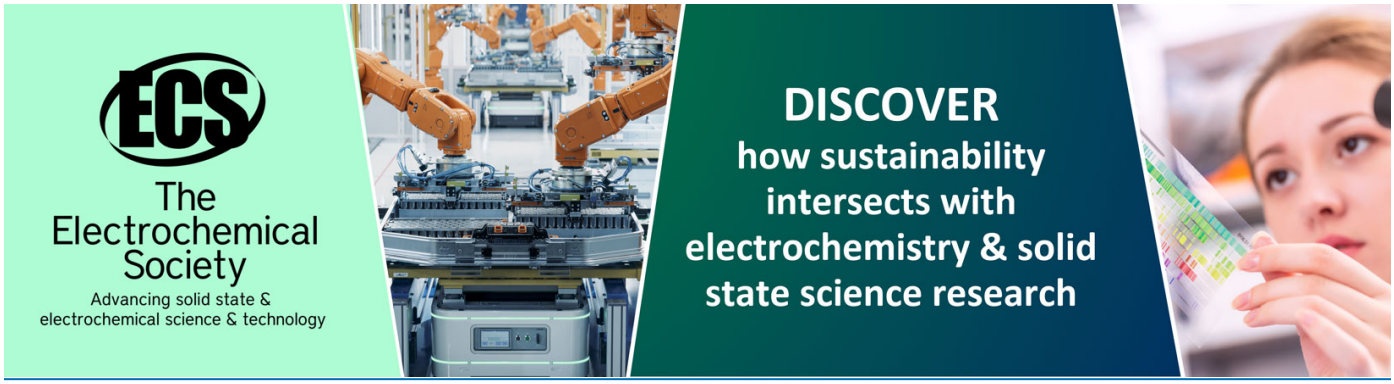

This content was downloaded from IP address 3.144.86.134 on 05/05/2024 at 19:38

IOP Conf. Series: Journal of Physics: Conf. Series **941** (2017) 012079 doi:10.1088/1742-6596/941/1/012079

Features of formation and evolution of crystal and local structures in nanocrystalline $Ln_2Zr_2O_7$ (Ln = La - Tb)

V V Popov[1,2], A P Menushenkov[2], B R Gaynanov[2], Ya V Zubavichus[1], R D Svetogorov[1], A A Yastrebtsev[2], A A Pisarev[2], L A Arzhatkina[3], K V Ponkratov[4]

[1]NRC "Kurchatov Institute", pl. Akademika Kurchatova 1, 123182 Moscow, Russia
[2]National Research Nuclear University MEPhI (Moscow Engineering Physics Institute), Kashirskoe sh. 31, 115409 Moscow, Russia
[3]JSC "Scientific Research Institute of Chemical Technology", Kashirskoe sh. 33, 115309 Moscow, Russia
[4]Renishaw plc, Kantemirovskaya st.58, 115477 Moscow, Russia

E-mail: BRGaynanov@gmail.com

Abstract. The formation of nanocrystal powders of $Ln_2Zr_2O_7$ (Ln=La - Tb) compounds upon calcinations up to 1500°C has been investigated by using of X-ray absorption fine structure spectroscopy combined with X-ray powder diffraction and Raman spectroscopy. It was found that the fluorite-pyrochlore phase transition occurs at calcination temperature in the range of 900-1200 °C (except Tb, T~1500 °C). The appearance of the ordered pyrochlore structure at calcination temperatures above 900 °C was fixed as an observation of superlattice peaks in diffraction and splitting of the first oxygen coordination shell in the local lanthanides environment in EXAFS and Raman spectra. In addition the scheme of fluorite-pyrochlore transition temperature dependence on radii of lanthanide cations was constructed.

1. Introduction

Rare-earth zirconates $Ln_2Zr_2O_7$ (Ln=La-Tb) have received considerable attention in recent years [1-5]. These systems contain several phases: pyrochlore (*Fd*-3*m*), fluorite (*Fm*-*3m*) types of crystalline structure and a phase with rhombohedral structure (*R*-*3*), formulated as $Ln_4M_3O_{12}$ [6]. The thermodynamic stability of the pyrochlore type compounds can be determined using empirical rule, which identifies the effective radii ratio $\gamma = r_{Ln3+}/r_{M4+}$ of REE and metal ions ratio as $1.46 < \gamma < 1.78$ [1]. Earlier we investigated and refined the temperature dependence of the fluorite-pyrochlore phase transition in a "boundary" zirconates $Dy_2Zr_2O_7$ ($\gamma = 1.43$) [7-8], $Gd_2Zr_2O_7$ ($\gamma = 1.46$) [9] and $Pr_2Zr_2O_7$ ($\gamma = 1.56$) [10].

The aim of the present work is to study the crystallization processes of an amorphous precursor upon isothermal calcination and to study the specific features of fluorite - pyrochlore phase transition in $Ln_2Zr_2O_7$ (Ln=La-Tb) (γ=1.44-1.61), using combined X-ray diffraction (XRD), X-ray absorption fine structure spectroscopy (EXAFS) at synchrotron radiation and Raman spectroscopy.

2. Experimental section

Content from this work may be used under the terms of the Creative Commons Attribution 3.0 licence. Any further distribution of this work must maintain attribution to the author(s) and the title of the work, journal citation and DOI.
Published under licence by IOP Publishing Ltd

The starting materials were $Ln(NO_3)_3 \cdot 6H_2O$ (more than 99,8% pure), $ZrOCl_2 \cdot 8H_2O$ (99% pure). Precursor (mixed Ln-Zr hydroxide) was prepared by co-precipitation of metal salts solution with ammonia $NH_3 \cdot H_2O$ (analytical grade). The $Ln_2Zr_2O_7$ powders were prepared by isothermal calcination of amorphous precursors at 600-1500^{o}C for 3 h in air. A more detailed experimental procedure was described in Refs. [11-14].

X-ray diffraction investigations were carried out at the "Structural Materials Science" beamline of the Kurchatov synchrotron radiation source. The measurements were implemented in the Debye-Scherrer geometry (transmission mode) using an environment optimized for high quality experimental data: the distance the sample - detector - 200 mm; beam size 200×200 mm; the exposure time of 15-30 minutes, the wavelength λ = 0.68886 Å. Six series of $Ln_2Zr_2O_7$ compounds with Ln=La-Tb were examined. Each series included 8-10 samples obtained by calcination of initial precursor at different temperatures in a temperature range 600 – 1500^{o}C. The Rietveld full profile analysis of X-ray diffraction patterns was performed with the Jana2006 software [15].

EXAFS spectra of $Ln_2Zr_2O_7$ (Ln=La-Tb) above the L_3-Ln (for La 5483 eV) and *K*-Zr (17998 eV) absorption edges, were measured at i811 beamline of MAXLab (Lund, Sweden) and P65 beamline of DESY (Gamburg, Germany) in a transmission mode at room temperature. Processing and modeling of XAFS-spectra were carried out using the VIPER [16] and Demeter [17] program packages. The amplitudes and phases of photoelectron back scattering in the local environment of zirconium, REE and hafnium atoms were calculated by program FEFF-8.20 [18] using the crystal structure parameters of pyrochlore and fluorite, taken from the diffraction data for $Ln_2Zr_2O_7$ (where Ln= La-Tb).

The Raman spectra were collected on a inVia Reflex confocal Raman microscope (Renishaw) (laser λ_1=532 nm and λ_2=785 nm) at room temperature [19].

3. Results and discussion

XRD study showed that precursors $La_2O_3 \cdot 2ZrO_2 \cdot 12{,}6H_2O$ calcinated at temperatures below 800°C have the X-ray amorphous structure. An increase in the atomic number along the La-Tb series leads to a decrease in the crystallization temperature. However, structure can't be considered as completely disordered, since from one to several broad peaks were observed in the region 13-21^o of double Bragg angle. The increasing of the calcination temperature above 800 °C leads to appearance of about ten X-ray reflections on XRD patterns for all samples, which corresponds to the fluorite structure formation. Besides at the annealing temperature above 1000°C we observed the gradual narrowing of the diffraction reflexes and the appearance of superlattice peaks (Figure 1), which point to the increase of the structure ordering. This is also correlated with increase of crystallite size and decrease of microstrain values obtained from the analysis of the diffraction patterns (see Figure 2).

These superstructure reflections are substantially wider than the main peaks of the fluorite-type structure. It suggests that cationic ordering with formation of the pyrochlore phase upon calcination occurs inside the separate regions (nanodomains) distributed over well-crystallized fluorite matrix.

Using EXAFS spectroscopy we have studied the evolution of the $Ln_2Zr_2O_7$ (Ln=La-Tb) local atomic structure upon the gradual heat treatment from initially amorphous precursors to well-crystallized powders.

Figure 3 shows the Fourier transform moduli of L_3-Nd EXAFS-functions $\chi(k)k^2$ of $Nd_2Zr_2O_7$ powders calcinated at different temperatures. The first maximum at R~1.9 Å corresponds to the nearest oxygen coordination shell around Nd. For the sample calcination at 600 ^{o}C, which is still amorphous and for the samples calcination at temperatures <1000 ^{o}C with the distinct fluorite structure, the shoulder at ~2.2 Å on the right slope of the main peak is quite small. But with an increase of calcination temperature the oxygen coordination shell starts to split into two components.

The observed splitting peak corresponds to two shorter Nd-O(2) and six longer Nd-O(1) distances. The second large features at 3.1 Å and 3.5 Å include contributions from Nd-Zr and Nd-Nd interatomic bonds. Amplitude of this features increases significantly with calcination temperature and the position drifts to larger radius (Figure 3). This indicates gradual ordering of the overall crystal structure. At calcination temperature exceeding 1300^{o}C the peak shape and amplitude substantially stabilize, which

corresponds to the end of the pyrochlore structure formation. Analysis of EXAFS data showed that spectra for samples prepared at calcination temperature <800°C are well reproduced by the model of fluorite structure (Figure 4). However, at higher calcination temperatures the fluorite structure model can no longer provide an adequate simulation of EXAFS-function and the analysis was conducted using the pyrochlore structure model. Thus above 1000 °C there is clearly observed splitting of the Nd-O bond length (Figure 4). This directly points to the restructuring of the local oxygen environment of rare-earth ions as a result of the observed fluorite-pyrochlore phase transition.

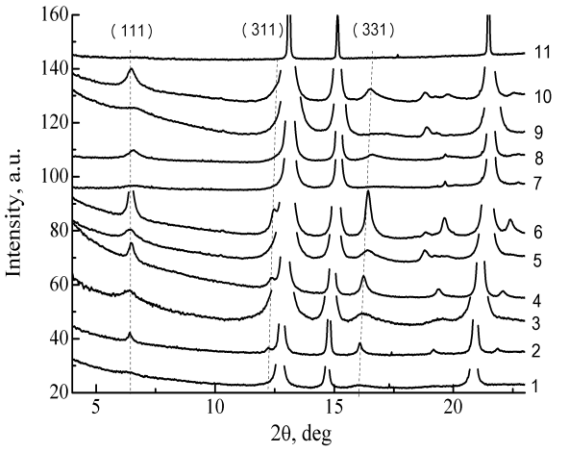

Figure 1. XRD patterns of $Ln_2Zr_2O_7$ powders obtained by precursor annealing in vicinity of the phase transition. Diffraction reflexes (111), (311) и (331) indicate presence of the pyrochlore phase. $La_2Zr_2O_7$ (1- 1000°C, 2- 1100°C), $Pr_2Zr_2O_7$ (3- 1000°C, 4- 1100°C), $Nd_2Zr_2O_7$ (5- 1100°C, 6- 1200°C), $Sm_2Zr_2O_7$ (7- 1100°C, 8- 1200°C), $Eu_2Zr_2O_7$ (9- 1100°C, 10- 1200°C), $Tb_2Zr_2O_7$ (11- 1500°C).

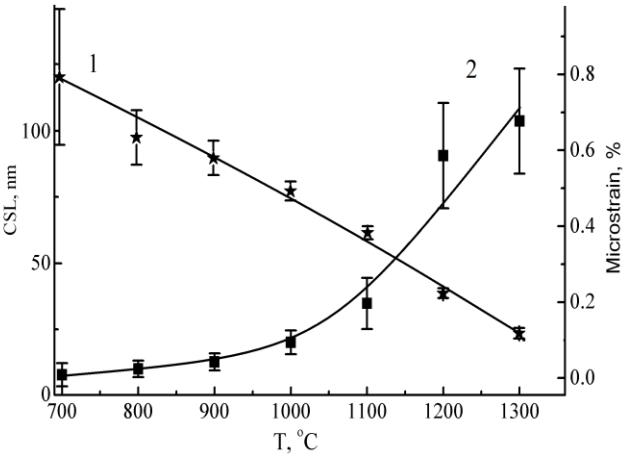

Figure 2. Microstrains (1) and coherent scattering lengths (2) of the series $Eu_2Zr_2O_7$ established by Rietveld method. Similar results were obtained for other Ln compounds.

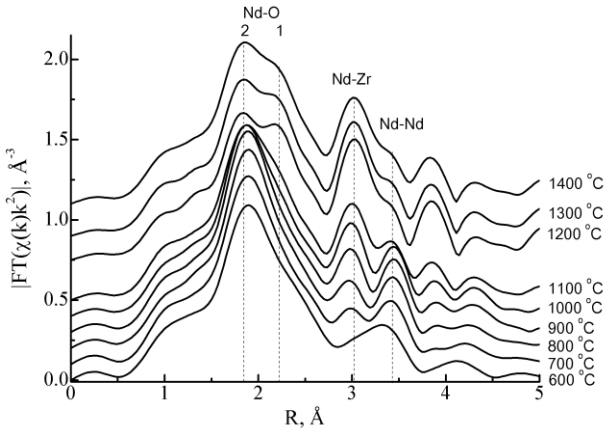

Figure 3. Fourier transform moduli of EXAFS experimental spectra measured above the L_3-Nd edge for $Nd_2Zr_2O_7$ calcinatated at different temperatures.

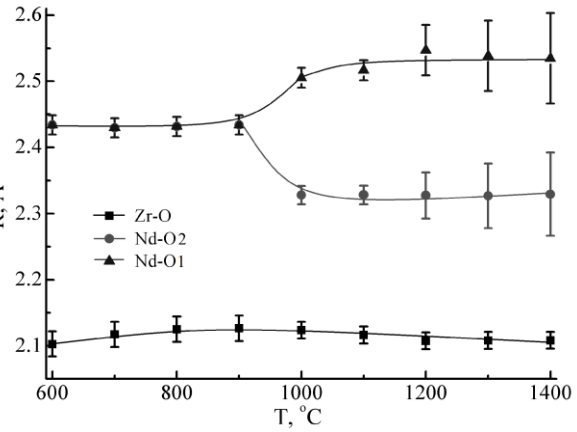

Figure 4. Figure 4. The interatomic bond lengths Nd-O and Zr-O in $Nd_2Zr_2O_7$ extracted from the EXAFS date.

Also, we have conducted a Raman spectroscopy study for each series of samples $Ln_2Zr_2O_7$. The effect of the type of rare-earth ions on the Raman spectra is represented in Figure 5. As seen in Figure 5,

Raman mode peaks for compounds from La to Tb become wider and shift to higher wavenumbers. Thus the most intense F_{2g} mode (~305 cm^{-1}) in the Raman spectra of $Tb_2Zr_2O_7$ is approximately one order of magnitude broader than that of $La_2Zr_2O_7$.

The results of our complex study of the phase transition in the $Ln_2Zr_2O_7$ series using EXAFS, XRD and Raman spectroscopy methods are summarized in Figure 6. EXAFS curve shows the beginning of the fluorite-pyrochlore transition, while Raman data point to the end. The initial crystallization of amorphous precursors leads to the formation of nanocrystalline oxides with the fluorite structure, regardless the Ln^{3+} cation type. The crystallization onset temperature is lower for $Ln_2Zr_2O_7$ with a smaller Ln^{3+} cation radius (or γ ratio). In contrast, the fluorite-pyrochlore phase transition temperature becomes higher across the $Ln_2Zr_2O_7$ series.

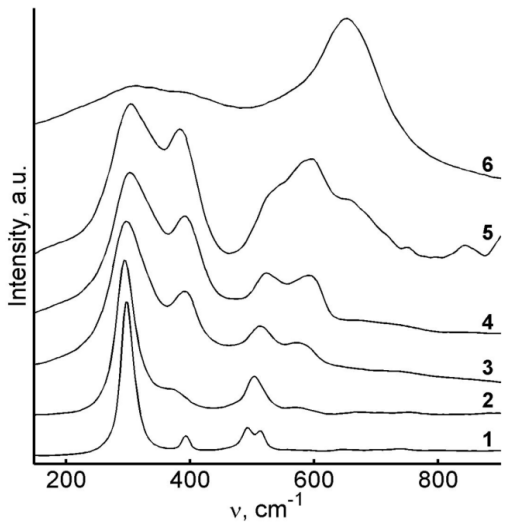

Figure 5. Raman spectra of $Ln_2Zr_2O_7$ (Ln=1-La, 2-Pr, 3-Nd, 4-Sm, 5-Eu, 6-Tb) powders with calcination temperature 1400 ^{0}C measured using 532 nm excitation.

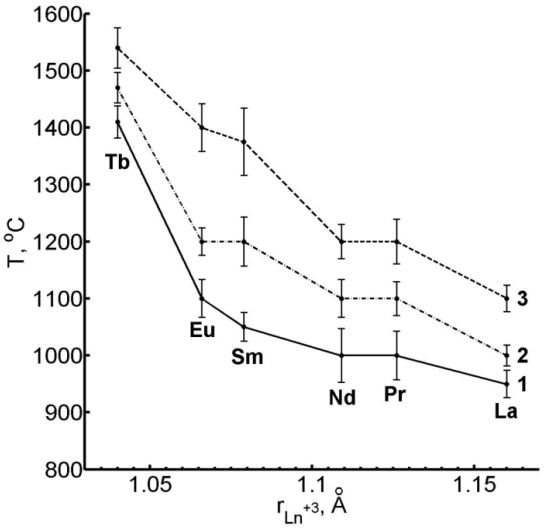

Figure 6. Scheme of the phase transition temperature for $Ln_2Zr_2O_7$ (Ln=La-Tb) compounds obtained from EXAFS-data analysis (1), XRD (2) and Raman spectra (3).

4. Conclusion

Local and crystal structure evolution of $Ln_2Zr_2O_7$ (Ln = La-Tb) upon the initial X-ray amorphous precursors calcination in the temperature range 600 – 1600 °C has been studied by using a combination of X-ray powder diffraction, XAFS-spectroscopy at synchrotron radiation and Raman spectroscopy. It was found that the fluorite-pyrochlore phase transition occurs at calcination temperature in the range of 900-1200 °C. The appearance of the ordered pyrochlore structure at calcination temperatures above 900 °C was fixed as an observation of superlattice peaks in diffraction and splitting of the first oxygen coordination shell in the local lanthanides environment in EXAFS and Raman spectra. Although X-ray diffraction data does not show crisp signs of superstructure in $Tb_2Zr_2O_7$, the results of the EXAFS data analysis show traces of pyrochlore ordering also in this boundary compound calcinated at 1500 °C.

Characteristic temperatures for the ordering in the cationic and anionic sublattices are slightly different (lower for the anionic sublattice) but both temperatures increase with decreasing of Ln^{3+} cation radius (or γ ratio). It was shown that the phase transition from fluorite to pyrochlore structure for Ln = La-Tb proceeds via the intermediate emergence and gradual growth of pyrochlore-type nanodomains in a fluorite matrix. In addition the scheme of fluorite-pyrochlore transition temperature dependence on radii of lanthanide cations was constructed.

Acknowledgements
The present work was supported by the Ministry of Education and Science of the Russian Federation (grant No 3.9750.2017/8.9).

References

[1] Subramanian M, Aravamudan G, Subba Rao G 1983 *Prog. Solid State Chem.* **15** 55
[2] Shamblin J, Feygenson M, Neuefeind J, Tracy C, Zhang F, Finkeldei S, Bosbach D, Zhou H, Ewing R, Lang M 2016 *Nat. Mater*. **15** 507
[3] Blanchard P, Clements R, Kennedy B, Ling C, Reynolds E, Avdeev M, Stampfl V, Zhang Z, Jang L-Y 2012 *Inorg. Chem.* **51** 13237-44.
[4] Karthik C, Anderson T, Gout D, Ubic R 2012 *J. Solid State Chem.* **194** 168
[5] Blanchard P, Liu S, Kennedy B, Ling C, Avdeev M, Aitken J, Cowie B, Tadich A 2013 *J. Phys. Chem. C* **117** 2266
[6] Andrievskaya E R 2008 *J. Eur. Ceram. Soc.* **28** 2363
[7] Popov V V, Menushenkov A P, Yastrebtsev A A, Zubavichus Ya V, Svetogorov R D, Kolyshkin N A 2016 *J. Phys.: Conf. Ser.* **747** 012042(1)
[8] Popov V V, Menushenkov A P, Zubavichus Ya V, *et al.* 2015 *Russ. J. Inorg. Chem*. **60** 16-22
[9] Popov V V, Zubavichus Ya V, Menushenkov A P, Yaroslavtsev A A, Kulik E S, Petrunin V F, Korovin S A and Trofimova N N 2014 *Russ. J. Inorg. Chem*. **59** 279
[10] Menushenkov A P, Popov V V, Gaynanov B R, Zubavichus Y V 2016 *J. Phys.: Conf. Ser.* **747** 012038(1)
[11] Popov V V 2015 *Russ. J. Inorg. Chem*. **60** 420
[12] Popov V V, Zubavichus Ya V, Petrunin V F, Menushenkov A P, Kashurnikova O V, Korovin S A, Chernikov R V and Yaroslavtsev A A 2011 *Glass Phys. Chem.* **37** 512
[13] Popov V V, Petrunin V F, Korovin S A, *et al.* 2011 *Russ. J. Inorg. Chem*. **56** 1538(10)
[14] Popov V V, Menushenkov A P, Zubavichus Ya V, *et al.* 2013 *Russ. J. Inorg. Chem*. **58** 1400(12).
[15] Petricek V, Dusek M, Palatinus L 2014 *Z. Kristallogr.* **229** 345
[16] Klementiev K V 2001 *J. Phys. D: Appl. Phys.* **34** 209
[17] Ravel B, Newville M 2005 *J. Synchr. Rad.* **12** 537
[18] Newville M 2001 *J. Synchr. Rad.* **8** 322
[19] Popov V V, Menushenkov A P, Yaroslavtsev A A, Zubavichus Ya V, Gaynanov B R, Yastrebtsev A A, Leshchev D S and Chernikov R V 2016 *J. Alloys Compd.* **689** 669